
Article:
Gineyts, E., Bonnet, N., Bertholon, C. et al. (17 more authors) (2018) The C-terminal intact forms of periostin (iPTN) are surrogate markers for osteolytic lesions in experimental breast cancer bone metastasis. Calcified Tissue International, 103 (5). pp. 567-580. ISSN 0171-967X

https://doi.org/10.1007/s00223-018-0444-y

The C-terminal intact forms of periostin (iPTN) are surrogate markers for osteolytic lesions in experimental breast cancer bone metastasis

Evelyne Gineyts[a,b], Nicolas Bonnet[c], Cindy Bertholon[a,b], Marjorie Millet[a,b], Aurélie Pagnon-Minot[d], Olivier Borel[a,b,g], Sandra Geraci[a,b], Edith Bonnelye[a,b], Martine Croset[a,b], Ali Suhail[e], Cristina Truica[e], Nicholas Lamparella[e], Kim Leitzel[e], Daniel Hartman[d,f], Roland Chapurlat[a,b,g], Allan Lipton[e], Patrick Garnero[a,b], Serge Ferrari[c], Philippe Clézardin[a,b,*], Jean-Charles Rousseau[a,b,*]

[a] INSERM, UMR 1033, Lyon, France; [b] Univ. Lyon, UFR de Médecine Lyon-Est, Lyon, France; [c] Division of Bone Diseases, Geneva University Hospital, Geneva, Switzerland; [d] Novotec, Lyon, France; [e] Penn State Hershey Medical Center, Hershey, PA, USA; [f] UMR CNRS 5510/MATEIS, Lyon, France; [g] Rheumatology Department, Hôpital Edouard Herriot, Hospices Civils de Lyon, Lyon, France

* These authors contributed equally to this work.

Running title: Periostin and breast cancer bone metastasis

To whom Correspondence should be addressed: Jean-Charles Rousseau, INSERM 1033, Pavillon F, Hôpital Edouard Herriot, Lyon 69437, France, Telephone : +33-4-72-11-74-86; FAX: +33-4-72-11-74-32; E-mail: jean-charles.rousseau@inserm.fr

ABSTRACT

Periostin is an extracellular matrix protein that actively contributes to tumor progression and metastasis. Here, we hypothesized that it could be a marker of bone metastasis formation. To address this question, we used two polyclonal antibodies directed against the whole molecule or its C-terminal domain to explore the expression of intact and truncated forms of periostin in the serum and tissues (lung, heart, bone) of wild-type and periostin-deficient mice. In normal bones, periostin was expressed in the periosteum and specific periostin proteolytic fragments were found in bones, but not in soft tissues. In animals bearing osteolytic lesions caused by 4T1 cells, C-terminal intact periostin (iPTN) expression disappeared at the invasive front of skeletal tumors where bone-resorbing osteoclasts were present. In vitro, we found that periostin was a substrate for osteoclast-derived cathepsin K, generating proteolytic fragments that were not recognized by anti-periostin antibodies directed against iPTN. In vivo, using an in-house sandwich immunoassay aimed at detecting iPTN only, we observed a noticeable reduction of serum periostin levels (-26%; $P < 0.002$) in animals bearing osteolytic lesions caused by 4T1 cells. On the contrary, this decrease was not observed in women with breast cancer and bone metastases when periostin was measured with a human assay detecting total periostin. Collectively, these data showed that mouse periostin was degraded at the bone metastatic sites, potentially by cathepsin K, and that the specific measurement of iPTN in serum should assist in detecting bone metastasis formation in breast cancer.

Keywords: periostin, bone metastases, cathepsin K, ELISA sandwich, breast cancer

INTRODUCTION

Bone metastases, the spread of cancer to the bones, are most commonly associated with cancers of the prostate, lung, and breast [1]. In bone metastasis, metastatic cancer cells disrupt the physiological balance between osteoclast-mediated bone resorption and osteoblast-mediated bone formation, resulting in bone destruction and release of bone matrix-derived factors that stimulate tumor growth [1-3]. Biochemical markers of bone resorption and bone formation, which are released as a result of malignant bone involvement, have demonstrated limited clinical utility for predicting bone disease progression and risk of skeletal-related events in patients with bone metastases [4, 5]. Consequently, the development of new markers detecting bone relapse is needed.

Periostin belongs to a family of extracellular matrix proteins including thrombospondins, secreted protein acidic and rich in cysteine (SPARC), osteopontin, and tenascin that regulate biological functions during embryonic development, tissue injury and cancer development, while these proteins are absent in almost all normal healthy adult tissues [6-8]. In cancer, periostin is usually expressed by fibroblasts associated with the tumor stroma where it promotes tumor cell adhesion and invasion through interactions with extracellular matrix proteins (tenascin C, fibronectin, type I collagen), cell surface receptors (integrins), and proteoglycans (heparin) [6]. This gain of adhesiveness and invasiveness induced by periostin expression confers to tumor cells a selective advantage during lung metastasis formation [9, 10]. In normal bone biology, periostin is preferentially expressed by osteoblasts and osteocytes in periosteum and cortical bone, respectively [11]. Periostin deficient mice develop periodontitis and osteoporosis [12]. It is an important mediator of cortical bone response to parathyroid hormone (PTH) and mechanical stress [11, 13, 14]. In bone metastasis, tumor cells create a permissive and supportive stroma environment for their growth [1-3]. Because periostin actively contributes to tumor growth [6, 9, 10], we hypothesized that it could be a useful marker for the detection of bone metastasis formation. To address this question, we first characterized antibodies directed against circulating and tissue-derived forms of mouse periostin, then developed a sandwich immunoassay with these antibodies for the sole detection of iPTN. Using this immunoassay, serum periostin levels were measured in an animal model of breast cancer bone metastasis**.** In parallel, we measured periostin in women with breast cancer and bone metastases with a human periostin assay detected total periostin in serum. Our study shows that mouse periostin is cleaved at bone metastatic sites, potentially by cathepsin K, and that the specific measurement of iPTN in serum should assist in detecting bone metastasis formation in breast cancer.

MATERIAL AND METHODS

1. Patient population and measurement of total periostin in human serum

A cohort of 53 women with metastatic hormone receptor-positive (or unknown) breast cancer and bone metastasis [mean age ± standard deviation (SD): 68.3 ± 11.03 years] and a control cohort of 54 age-matched healthy post-menopausal women were used for periostin serum measurements [15]. Blood was drawn 14 days before initiation of therapy. Serum was stored at -80°C until use. Circulating levels of periostin in patients were measured using a commercial sandwich Enzyme-linked immunosorbent assay **(**ELISA) kit (USCN, China), as previously described [16].

2. Animal studies

The animals were maintained in a 12 hrs light-dark cycle and given free access to food and water. All procedures involving animals, including their housing and care, the method by which they were culled, and experimental protocols were reviewed and approved by local ethical committees of Geneva School of Medicine (Geneva, Switzerland) and the University of Lyon (Lyon, France)**.** Animal studies were routinely inspected by the attending veterinarian to ensure continued compliance with the proposed protocols.

Postn$^{-Lac\ Z}$ knock-in C57Bl6/J mice (Postn$^{-/-}$) and wild-type mice (Postn$^{+/+}$) were generated as previously reported [17]. Serum and tissues (bone, lung and heart) were collected for biochemical analyses. Bone metastasis experiments were conducted using 5 week-old immunocompetent female Balb/c mice (Charles River, France). Mouse 4T1 breast cancer cells [5 x 10^5 cells in 0.1ml of phosphate buffered saline (PBS)] or only PBS (naïve group) were inoculated intra-arterially to animals. The formation of osteolytic lesions was monitored by radiography, using a cabinet X-ray system (Faxitron, USA). Osteolytic lesions were identified on radiographs as radiolucent lesions in bone. Animals were sacrificed on day 14 after tumor cell inoculation. The hind limbs were collected for immunohistochemistry (IHC). Serums were stored at -80°C until used for iPTN measurements.

3. Antibodies against mouse periostin

Rabbit antibodies used are (i) a biotin-conjugated polyclonal antibody (Ab1) (BAF-2955, R&D, USA) and (ii) an in-house polyclonal antibody (Ab2) directed against amino-acid sequences 790-811 of mouse periostin, respectively. Ab2 antibody was obtained by immunizing New Zealand White rabbits using a synthetic peptide (**KKIPANKRVQGPRRRSREGRSQ**, Genepep, France) coupled to keyhole limpet hemocyanin. All spliced variants of periostin share the amino-acid sequences recognized by Ab1 and Ab2 antibodies meaning that in the next

immunoblotting analyses the bands recognized by both Ab1 and Ab2 antibodies correspond to iPTN and the bands recognized only by Ab1antibody correspond to cleaved periostin at the C-terminal end.

4. Preparation of mouse serum

Serum (25µl) was depleted of three high abundant proteins [albumin, immunoglobulin G (IgG) and transferrin] using a MARS Ms-3 cartridge (Agilent technologies, USA). Proteins were desalted by precipitation using 2-D Clean-Up kit (GE-Healthcare-Life-Sciences, Germany), according to the manufacturer's instructions. Thereafter, proteins were rehydrated with 25µl of Laemmli sample buffer (Bio-Rad, USA) or 25µl of Destreak rehydration solution (GE-Healthcare-Life-Sciences, Germany) for one-dimensional (1D) or two-dimensional (2D) electrophoresis, respectively.

5. Preparation of mouse tissue extracts

The proximal and the distal metaphysis of femora were removed and the bone marrow was flushed out. Bones and lungs of mice were extensively washed with demineralized water and then ground to fine powder in liquid nitrogen. Proteins were extracted from tissue powder using 7 M urea, 2 M thiourea, 4% 3-[(3-cholamidopropyl)dimethylammonio]-1-propanesulfonate (CHAPS), 20mM 1,4-dithiothreitol (DTT), 1% immobilized pH gradient (IPG) buffer pH 3-10 (GE-Healthcare-Life-Sciences, Germany), desalted and concentrated by precipitation using 2-D Clean-Up kit. Proteins were rehydrated with Destreak rehydration solution and quantified using 2-D Quant kit (GE-Healthcare-Life-Sciences, Germany).

6. Electrophoresis and Immunoblotting

For 1D electrophoresis, non-reduced or reduced, 5µl of depleted serum were loaded on 7.5% Mini-PROTEAN® TGX™ Precast Protein Gels, 10-well, 30µl (Bio-Rad, USA) and electrophoresed at 200 volts with Mini-Protean® Tetra Vertical Electrophoresis system (Bio-Rad, USA).

For 2D electrophoresis, 60µg of protein tissue extracts or 12.5µl of depleted serum were diluted to a final volume of 125µl in a Destreak solution buffer supplemented with 20mM DTT and 1% IPG buffer pH 3-10. IPG strips, 7 cm, pH 3-10L (GE-Healthcare-Life-Sciences, Germany) were rehydrated with the samples during 18h at 20°C. The isoelectric focusing (IEF) was carried out using an Ettan IPGphor II IEF Unit (GE-Healthcare-Life-Sciences, Germany) for 4.5 hrs with a gradient of 500 to 4000 volt-hrs. After IEF, IPG strips were first reduced in a buffer containing 6M urea, 50mM Tris–HCl, pH 8.8, 2% sodium dodecyl sulfate (SDS), 30% glycerol and 0.002% bromophenol blue supplemented with 10mg/ml DTT, and then alkylated using the same buffer supplemented with 25 mg iodoacetamide (GE-Healthcare-Life-Sciences, Germany). The procedure was done at room temperature for 15 min with each

component (DTT and iodoacetamide). Reduced and alkylated IPG strips were then placed on 7.5% Mini-PROTEAN® TGX™ Precast Protein Gels, 7cmm IPG/prep well, 450µl (Bio-Rad, USA) and then proteins were electrophoresed at 110 volts.

After electrophoresis, proteins were transferred onto nitrocellulose membranes with iBlot Dry Blotting System (ThermoFisher Scientific, USA) and analyzed by immunoblotting. Membranes were probed with rabbit anti-periostin Ab1 or Ab2 polyclonal antibody (1: 1,000 dilution) or with a mouse monoclonal antibody (5µg/ml concentration) that is directed against γ-carboxylation modification of glutamic acid (Gla) residues (Sckisui Diagnostics LLC, USA). After overnight incubation with primary antibodies at 4°C, membranes were washed then incubated 1 hr at room temperature with horseradish peroxidase (HRP)-conjugated donkey anti-rabbit (1:8000 dilution) or HRP-conjugated goat anti-mouse secondary antibody (1: 8,000 dilution) (Jackson ImmunoResearch, UK), and immunostaining was performed with a Chemiluminescence Imaging System (Chemi-Smart 2100WL/20M, Vilber Lourmat, Germany).

7. IHC

Hind limbs were fixed in alcohol, formalin, and acetic acid fixative, decalcified with Osteosoft solution (Merck KGaA, Germany), dehydrated and paraffin-embedded. Bone tissue sections were incubated overnight at 4°C with rabbit polyclonal Ab1, Ab2 (1: 1,000 dilution) and cathepsin K antibody (1: 100 dilution, Biovision Inc., USA). After washing, bone tissue sections were incubated 1 hr at room temperature with an HRP-conjugated donkey anti-rabbit secondary antibody (1: 100 dilution; GE-Healthcare-Life-Sciences), and the signal developed with diaminobenzidine (Dako product, Agilent Technologies, InC., USA). Additionally, osteoclasts within bone tissue sections were stained using the tartrate-resistant acid phosphatase (TRAP) activity kit assay (Merck KGaA, Germany).

8. Development of an ELISA assay against mouse iPTN

All steps of this protocol were performed under shaking conditions (450 rpm). Streptavidin-coated plates (Nunc Immobilizer, Dutscher, France) were first washed 3 times with Tris-buffered saline (TBS) containing 0.05 % Tween-20 (Euromedex, France). Then plates were coated with Ab1 antibody (200 µl/well; 200 ng/ml) in TBS containing 0.5% bovine serum albumin [(BSA), Euromedex, France] and 10 mM $CaCl_2$ (Merck KGaA, Germany) (Assay buffer), for 2h at room temperature. After washing with TBS containing 0.5% BSA and Tween-20 (washing buffer), 50 µl/well of zero calibrators (assay buffer), calibrators (serial dilutions of the recombinant mouse periostin [R&D System, Inc., USA] in assay buffer), quality controls and unknown sera (diluted to 1:40 in assay buffer) were incubated overnight

with Ab2 antibody (100 µl/well; 16 ng/ml diluted in assay buffer) at 4°C. The unbound material was eliminated by washing. Then, HRP–conjugated antibody diluted to 1: 8,000 in assay buffer was added (100 µl/well) for 1 hr at room temperature. After a final wash, 100 µl/well of substrate solution [3,3',5,5' tetramethylbenzidine, (TMB), Euromedex, France] was added for 30 min and the reaction was stopped by the addition of 100 µl/well of 0.2 M sulfuric acid (Merck KGaA, Germany). Optical density (OD) was measured at a wavelength of 450 nm, corrected for absorbance at 620 nm. Unknown values were calculated using a five-parameter curve fitting procedure (Ascent™ Software for Multiscan, ThermoFisher Scientific, USA). All measurements were performed in duplicate.

9. Cathepsin K digestion and Liquid chromatography-tandem mass spectrometry (LC-MS/MS) analysis

Mouse recombinant periostin (1.1 µM) was digested with cathepsin K **(**Enzo, France**)** (2.2 µM) at 20°C (substrat/enzyme ratio: 0.01, 0.1, 0.5, 1, 1.5, 2). After 1 hr incubation, cathepsin K inhibitor E64 (250 µM) (Merck KGaA, Germany) was added to stop the digestion. The different digested periostin samples obtained were either used for immunoblotting detection, or LC-MS/MS analysis or ELISA measurement. Periostin proteolytic fragments were then separated by 1D electrophoresis on 4-20% Mini-PROTEAN® TGX™ Precast Protein Gels, 10-well, 30µl (Bio-Rad, USA), at 200 volts and immunoblotted with Ab1 or Ab2 antibodies or stained with Bio-Safe TM Coomassie G-250 (Bio-Rad, USA). The 25-kDa Coomassie-blue-stained proteolytic band was excised, digested with trypsin and peptides sequenced on LTQ Velos and Qstar XL Mass Spectrometers (ThermoFisher Scientific, USA).

10. Statistical analysis

All data were analyzed using StatView software (SAS, USA). Results are reported as mean ± SD. Pairwise comparisons were carried out by performing a nonparametric Mann-Whitney U test. P values less than 0.05 were considered statistically significant.

RESULTS

1. Circulating periostin levels in breast cancer patients with bone metastases (Fig. 1)

Periostin levels were measured in the serum of breast cancer patients with bone metastases (n = 53) and compared to that observed in the serum of healthy individuals (n = 54), using a sandwich ELISA kit with a polyclonal antibody (AbH) that is directed against the first fasciclin-like domain (FAS I) of human periostin, which is common to all periostin isoforms (Fig.1A). Serum periostin levels did not significantly differ between women with breast cancer and bone metastasis and those from aged-matched healthy post-menopausal women (-6%, 3272 ± 1043 vs 3489 ± 1015 ng/ml, P=0.18) (Fig. 1B).

2. Biochemical characterization of mouse periostin in serum, bone and soft tissues (Fig. 2 and 3)

We used two polyclonal antibodies against mouse periostin, one being commercially available and directed against amino-acid sequence 24-811 (Ab1) and the second one (Ab2) was developed in our laboratory and directed against the last C-terminal 22 amino acids (790-811) (Fig. 2A). All spliced variants of periostin share the same amino-acid sequence recognized by Ab1 (first FAS-I domain) and Ab2 (last 22 C-terminal amino acids) antibodies, thereby allowing the detection of all periostin isoforms. Ab1 and Ab2 antibodies were first used to identify periostin by immunoblotting after separation of protein extracts from mouse sera by 1D electrophoresis (Fig. 2B). When proteins were electrophoresed under non-reducing conditions (-DTT), Ab1 and Ab2 antibodies recognized the same 250-kDa protein band in the serum from C57Bl6/J normal mice (Fig. 2B). This 250-kDa band disappeared under reducing conditions (+DTT), while several bands, including a strongly stained 75-kDa doublet band, were immunodetected by Ab1 antibody (Fig. 2B). Ab2 antibody only recognized the upper band of this doublet (Fig. 2B). Importantly, these protein bands were not immunodetected in the serum of Postn$^{-/-}$ mice (Fig. 2B), demonstrating the specificity of Ab1 and Ab2 antibodies against periostin. These bands likely represented polypeptides closely related in structure, suggesting a mixture of intact and proteolytic forms of periostin. To further address this question, serum proteins were electrophoresed and transferred to a nitrocellulose membrane, then a single lane was split in half, each half was blotted separately with antibodies Ab1 and Ab2, and the two halves were matched prior to imaging. As shown in Fig. 2C, under reducing conditions (+DTT), Ab2 antibody only stained the upper molecular-weight band whereas both bands were stained with Ab1 antibody. Proteins extracted from the serum, and bone and soft tissues (lung and heart) of wild-type and Postn$^{-/-}$ mice were then subjected to 2D electrophoresis, transferred to nitrocellulose membranes and probed

with Ab1 or Ab2 antibody. As shown in Fig. 3, irrespective of the protein source, Ab1 and Ab2 antibodies detected an array of spots with molecular weights at about 75 kDa. However, isoelectric points (pI) of Ab1-positive spots ranged mainly between 6 and 7 (Fig. 3, panel A, $Postn^{+/+}$, box 1), whereas those of Ab2-positive spots ranged essentially between 7 and 9 (Fig. 3, panel B, $Postn^{+/+}$, box 2) (see spot details with area magnification, Fig. 3, panel C). Moreover, Ab1 antibody specifically recognized an array of spots at 37 kDa in bone, but not in the serum and soft tissues (lung and heart) of $Postn^{+/+}$ mice, that likely represented proteolytic fragments of periostin (Fig. 3, panel A, $Postn^{+/+}$, bone, box 3). Other spots detected by Ab1 and Ab2 antibodies in the serum and tissues of $Postn^{+/+}$ mice were nonspecific, since these spots were also detected in the serum and tissues of $Postn^{-/-}$ mice (Fig. 3; arrows).

3. Periostin is not a γ -carboxylated protein (Fig. 4)

It has been previously reported that periostin is a vitamin K-dependent γ-carboxylated protein [18]. To analyze for the presence of γ-carboxylation, proteins extracted from the serum and bone and lung tissues were subjected to 2D electrophoresis, transferred to nitrocellulose membrane and probed by immunoblotting using a monoclonal antibody specific for Gla residues. As shown in Figure 4, there was no overlap between Gla-positive spots and areas where periostin-positive spots were detected in the serum and lung (boxes 1 and 2) and in bone (boxes 1, 2 and 3) from $Postn^{+/+}$ mice. Additionally, similar Gla-positive spots were observed in the serum and tissues from $Postn^{-/-}$ mice while periostin was deleted. These data demonstrated that mouse periostin was not a γ-carboxylated protein, as proposed by Coutu et al. [18]. Similar findings were recently reported for human periostin [19]. Additionally, we verified in our immunoblotting conditions that the commercial monoclonal anti-Gla antibody recognized two well-known Gla proteins, the vitamin K-dependent protein C (9 Gla residues) and the coagulation factor IX (12 Gla residues). We observed a specific labeling at the expected molecular weights (62 kDa, and 55 kDa, respectively) and pI areas (4.4-4.8 and 4.2-4.5, respectively) (Supplemental Fig. S1).

4. In situ expression of periostin in normal and metastatic mouse bones (Fig. 5)

IHC of mouse bone tissue with Ab1 and Ab2 antibodies showed a strong expression of periostin in the periosteum, but not the endosteum (Fig. 5A arrows). In experimental bone metastasis caused by mouse 4T1 breast cancer cells, Ab1 immunostaining of bone metastatic tissue sections showed a strong stromal expression of periostin at the invasive front of the tumor, whereas Ab2 immunostaining was negative (Figs. 5B-Ab1 and -Ab2). Additionally, as judged by the TRAP and cathepsin K staining of bone tissue sections, this absence of Ab2 immunostaining localized at the tumor

bone interface where active-osteoclast resorption surfaces were present (Fig. 5B-TRAP and 5B-cathepsin K). Of note, both Ab1 and Ab2 antibodies still strongly stained the periosteum in normal bone areas at a distance from skeletal tumors (Fig. 5C, arrows), further indicating that the loss of immunoreactivity with Ab2 antibody was specifically associated with cancer-induced osteolysis.

5. In-house ELISA to measure iPTN in serum (Fig. 6A)

We developed a sandwich ELISA for the sole detection of iPTN forms, using Ab1 and Ab2 as the capture and detection antibodies, respectively. A typical standard curve is shown in Figure 6A. The intra- and inter-assay precisions of the immunoassay for serum were below 4 and 13%, respectively. The mean dilution recovery was 105 % and the mean spiking test was 99%, allowing accurate measurements of periostin from 1 to 50 ng/ml. The detection limit -defined as the concentration 2 standard deviations above that of the lowest calibrator- was <1 ng/ml. Serum periostin was stable for up to 5 thaw/freeze cycles and at least 2 hrs at room temperature. In addition, our immunoassay did not measure any circulating periostin levels in Postn$^{-/-}$ mice and it did not allow detection of human serum periostin (data not shown), demonstrating its specificity.

6. Association between serum periostin levels and bone metastasis in animals (Fig. 6B)

We next measured circulating levels of periostin from animals bearing metastatic osteolytic lesions caused by murine 4T1 breast cancer cells. Fourteen days after tumor cell inoculation, animals developed osteolytic lesions, as judged by radiography (Fig. 6B, inset and white arrows), at which time blood was collected for serum measurement of periostin levels. Compared to age-matched naïve animals (i.e., mice that did not receive 4T1 cells), there was a 26% decrease of periostin levels in the serum of metastatic animals (mean ± SD: 560 ± 100 vs 756 ± 64 ng/ml, $P<0.002$) (Fig. 6B).

7. Recombinant mouse periostin is a substrate for cathepsin K (Fig. 7)

Cathepsin K is a major cysteine protease in osteoclasts that plays a key role in osteoclast-mediated bone resorption [1]. We therefore tested the ability of cathepsin K to digest mouse recombinant periostin. As shown in Fig. 7A, cathepsin K generated at least four proteolytic fragments with molecular weights ranging from 75 to 25 kDa. These proteolytic fragments were detected by Ab1, but not Ab2 antibody. The 25-kDa proteolytic fragment of mouse periostin was a final degradation product (Fig. 7A; arrow and Supplemental Fig. S2). This Coomassie blue-stained proteolytic fragment was therefore sequenced by LC-MS/MS. The sequence analysis demonstrated the presence of N-terminal

fragments between amino acid residues Val97 and Glu377, which consisted mainly of the two first FAS I domains (amino acids: 99-367) of mouse periostin (Figure 7B). Thus, periostin is a substrate for cathepsin K with potential cleavage sites located in the N-terminal EMI domain and the C-terminal region encompassing the third and fourth FAS I domains (Fig. 7C). In addition, recombinant mouse periostin was treated with different ratio of cathepsin K / periostin (0.5, 0.1, 0.01). The resulting fragments were analyzed by 1D electrophoresis and immunoblotting with Ab1 or Ab2 antibodies. In parallel, remaining intact periostin (%) was measured with our in-house ELISA assay. The fragments of periostin generated by cathepsin K cleavage were not recognized on the immunoblot with Ab2 and were not measured by ELISA, demonstrating the specificity of our assay for iPTN (Fig. 7D).

Discussion

Origin of this study

We previously developed a competitive assay for the measurement of total circulating periostin in mouse using Ab2 antibody [20]. According to the location of the Ab2 epitope, the last C-terminal 22 amino-acids common to all periostin isoforms, this assay reflected stoichiometrically the expression of periostin. This epitope is mouse specific and consequently this assay is not adequate for human periostin measurements. We observed that serum periostin was markedly increased in metastatic mice inoculated with human B02 breast cancer cells suggesting that periostin could be a biochemical marker of the early stromal response associated to breast cancer bone metastasis [21].

Measurement of total periostin in human serum

In order to evaluate the relevance of this approach in human, we measured serum periostin levels in a cohort of women with breast cancer and bone metastasis with a commercial sandwich ELISA kit previously described [16, 22]. This assay used a polyclonal antibody (AbH) that is directed against the FAS-I of human periostin common to all periostin isoforms meaning that it also reflects stoichiometrically the expression of human periostin. As opposed to what was observed in mouse, periostin levels did not significantly differ between women with breast cancer and bone metastasis and healthy post-menopausal women. Our data suggested that the measurement of total periostin was not relevant in human.

It can be noted that Sasaki et al. showed that serum periostin levels were elevated in breast cancer patients presenting with bone metastases compared to similar breast cancer patients without evidence of bone metastasis [23]. As they used an in-house assay with 2 antibodies whose epitopes were not described we do not know which forms of periostin are recognized by this assay.

Characterization of periostin forms in serum and tissues from wild type mice

In order to develop a more relevant periostin assay, we analyzed the periostin forms present in the circulation and in the tissues of wild type mice. We demonstrated that periostin circulated only as disulfed multimers of 250 kDa. These multimers were composed of monomer forms, at least four, around 75 kDa detected differently by Ab1 and Ab2 antibodies. Those not recognized by Ab2 correspond to fragments cleaved in their C-terminal part. Those recognized

by both antibodies were rather under 80 kDa suggesting also a potential cleavage in the N-terminal part before the cysteine cluster responsible of disulfide bridges leading to multimers. Moreover, 2D electrophoresis showed that the periostin, in the tissues and in the serum, was a mixture of proteins distributed along a vertical axis according to their molecular weights as previously shown with 1D electrophoresis approach but also along a horizontal axis according to the difference of pI. We also noticed that the labeling between Ab1 and Ab2 was different with Ab2 recognizing only a part of protein spots detected by Ab1 with more basic pI (between 7 and 9). We verified the specificity of periostin spots using null mice serum. This was particularly useful for Ab2 because the presence of non-specific chain of spots found both in wild type and null mice serum. Interestingly, in bone Ab1 recognized specifically a serial of spots with a molecular weight around 37 kDa not highlighted by Ab2 suggesting the presence of smaller periostin fragments in bone cleaved at the C-terminus. These fragments were not detectable in the serum. Collectively, these results showed that the periostin is a complex family of proteins with a specific bone signature.

Periostin is not a γ-carboxylated protein

These chains of spots in the horizontal axis suggested a serial of post translational modifications for mouse periostin. Coutu et al. have shown that periostin from mesenchymal stromal cells could be γ-carboxylated but Annis et al. did not observe this phenomenon in human periostin from lung [18, 19]. Using the same antibody as in the Coutu et al. study, directed against Gla residues, we did not detected the periostin spots in serum and tissues demonstrating that the mouse periostin forms recognized by Ab1 and Ab2 antibodies were not γ-carboxylated. However, the antibody anti-Gla highlighted in serum and bone several acidic spots that were present both in wild type and null mice. These spots may correspond to the serum Gla proteins involved in blood coagulation (coagulation factors II, VII, IV and X, proteins C and S) and the well-known γ-carboxylated bone proteins osteocalcin (OC) and matrix-Gla-protein (MGP). One explanation of the discrepency with Coutu et al. could be that these authors used in vitro system with mesenchymal stromal cells stimulated by vitamin K. On the contrary, we used in vivo system with mouse serum and proteins extracted directly from tissues. The same approach was performed by Annis et al. using proteins extracted from fibrotic lungs [19]. Another post translational modification demonstrated for periostin is a N-glycosylation in amino acid 601 [24]. We could hypothesis that the horizontal chain of spots could be the result of a variable lenght of the sugar chain leading to different pI. Collectively, these results show that mouse periostin was not a γ-carboxylated in vivo.

Strategy for the development of a new assay

Using 1D and 2D electrophoresis, we found in mouse serum and tissues the presence of different forms of periostin. However, this approach does not highlight qualitative and quantitative differences concerning the circulating forms of periostin between control and mice inoculated with 4T1 breast cancer cells developing bone metastases (data not shown). Moreover, the IHC performed on metastatic bone tissue sections showed that Ab2, recognizing only iPTN, did not stain the desmoplastic tumor stroma adjacent to bone where active osteoclast-mediated bone resorption and cathepsin K was taking place (Fig. 5B), whereas it did stain the periosteum at a distance from the tumor (Fig.5C). The observation that Ab2 antibody could no longer bind to its epitopes at the tumor/bone interface was indicative of the proteolytic degradation of periostin specific for the bone metastatic process. Taken together, these data suggested that the specific measurement of cleaved periostin or intact forms could be more relevant in a context of bone metastases.

Sandwich assay development and preclinical evaluation

We developed a new assay with the 2 antibodies used for the previous immuno-chemical study with Ab1 as capture antibody and Ab2 as revelation antibody. According to this assay format and with the epitope locations, this pair of antibodies is able to detect only the intact forms of periostin. We showed that these intact forms were circulating as opposed to the bone fragments (see Figure 3, panel A, Postn$^{+/+}$, box 3, serum vs bone). Moreover, developing a sandwich assay eliminates all risks of non-specific recognition in serum as showed by the non-specific background observed with Ab2 in 2D electrophoresis analyses. Our assay demonstrated adequate technical performances with respect to precision, dilution of serum samples and specificity allowing the accurate measurement of serum mouse iPTN levels. We used a protocol with mice inoculated with 4T1 breast cancer cells developing bone metastases. We observed a significant decrease of iPTN serum levels in these animal compared to control mice (-26%) suggesting that the reduction of circulating iPTN was associated with occurrence of breast cancer osteolytic lesions in vivo.

Hypothesis for the serum decrease of iPTN in mice bearing bone metastases

This decrease of serum iPTN levels was concomitant to an intense labeling of metastatic areas in bone with Ab1 (Fig.5, panel B, Ab1). This IHC result is consistent with an overexpression of periostin in metastases as previously showed [21]. These differences between tissue expression and serum levels could be explained by a degradation of periostin by bone enzymes. In this regard, cathepsin K appears as a potential candidate. This is the most abundant degrading enzyme in bone and it is overexpressed in metastatic models [25]. We observed that recombinant periostin molecule was a substrate for cathepsin K in vitro generating large fragments not recognized by Ab2 meaning that the C-terminal

part was cleaved. We verified that these fragments were not detected in our assay**.** Cathepsin K deletion in animals leads to an upregulation of periostin in the periosteum during bone formation and increased serum levels of periostin in cathepsin-K deficient mice, as measured with our in-house assay [26]. Moreover, Garnero identified two major cleavage sites for cathepsin K located in the C-terminal part of human periostin [27]. The resulting peptide was measured in human serum and also detected in the mouse tibia cortical bone demonstrating that human and mouse periostin were both substrates for cathepsin K. This peptide (8 amino acids in bold letters) and the amino acids on both sides were highly conserved between human (IKVIE-**GSLQPIIK-**TEGPA) and mouse (IKVIQ-**GSLQPIIK-**TEGPA) sequences suggesting that the cleavage sites were active in both species. Interestingly, these cleavage sites were located 142/150 amino acids before the C-terminal end generating large fragments of periostin with reduced molecular weights of 14/15 kDa compared to iPTN. This difference was in the same order of magnitude than that observed in our immunoblotting experiments under reducing conditions (Figure 2C). In addition, IHC of metastatic bone tissue sections indicated the presence of osteoclasts and cathepsin K at the tumor/bone interface where the staining of Ab2 disappeared, further suggested that periostin cleavage was intense in this area (Figure 5B)**.** Taken together, these data suggested that periostin could be cleaved by cathepsin K at the tumor/bone interface.

Strenghts and limitations

The strenghts of our study include 1/ a global approach for the development of an assay including 2D electrophoresis analyses for the characterization of circulating periostin forms but also for the characterization of antibody recognition 2/ the highlighting of a periostin bone signature corresponding to periostin fragment cleaved in C-terminus and 3/ the development of a reliable periostin assay measuring specifically the intact forms of periostin showing a significant decrease of serum iPTN levels in animal bearing bone metastases compared to control mice.

However, we did not highlight qualitative modifications with 2D approach in relation with the quantitative differences observed by enzyme-linked immunosorbent assay in the animal protocol (data not shown). This could be due to the limits of separation of 2D mini-gel electrophoresis. We only have a bundle of indirect arguments suggesting the involvement of cathepsin K in the periostin cleavage. Firstly, the origin of cathepsin K is uncertain, it can come from osteoclasts but also 4T1 cancer cells [28-30]. Moreover, in the family of cysteine proteases, cathepsin B or L can also cleave mouse periostin [27]. Previous studies identified periostin as a substrate for matrix metalloproteinases (MMPs) MMP-3, MMP-12 and MMP-14 [31], the last two being expressed by mouse osteoclasts [32]. Proteolytic degradation

of periostin in bone metastasis could therefore also result from cleavage by MMP-12 or MMP-14. However, none of these MMPs were involved in bone matrix degradation [32], as opposed to cathepsin K in breast cancer and bone metastasis [33-36].

Additional studies are needed with other mouse models of osteolytic bone metastasis to evaluate if the reduction of iPTN is correlated to the early detection of bone metastases. Finally, proteolysis of periostin by circulating proteases in vivo and/or during sample handling ex vivo might also occur. We and others [37, 38] previously reported similar observations with the truncation of human osteocalcin, emphasizing the need of careful sampling conditions to generate reliable data.

Conclusion

Our findings underscore the importance of knowing the catabolism of bone proteins for the development of new immunoassays. Several different immunoassays for periostin measurement are commercially available. Serum periostin levels rely on the epitope recognized by the immunoassay and these epitopes are not known most of the time, so it is difficult to interpret data. Nevertheless, our study is the first one showing that the reduction of circulating levels of iPTN was associated with occurrence of breast cancer osteolytic lesions in animals. We hypothethize that this circulating decrease is due to cathepsin K cleavage. In the light of these experimental findings, we suggest that the specific serum measurement of iPTN should assist in detecting bone relapse in breast cancer patients.

Acknowledgments:

We thank Ms Madeleine Lachize and Juliette Cicchini for her technical assistance. We thank Dr Isabelle Zanella-Cleon and the team of the mass spectrometry platform facility (Protein Science Facility, SFR Biosciences UMS3444/US8) for LC-MS/MS sequencing of periostin proteolytic fragments.

Conflict of interest:

The authors declare that they have no conflicts of interest with the content of this article

Authors contributions:

Study design: JCR and PG. Study conduct: EG and JCR. Data collection: CB, MM, EG, OB, SG, EB, NB, MC, AS, CT, NL, KL. Data analysis: EG, JCR, CB, MM, OB, APM, SG, EB, NB. Data interpretation: EG, JCR, RC, PG, AL, DH, NB, SF and PC. Drafting manuscript: EG, JCR, and PC. All authors have read and approved the final version of the manuscript.

Supplemental data:

This article contains supplemental Figs. S1 and S2

Funding sources

This research did not receive any specific grant from funding agencies in the public, commercial, or not-for-profit sectors.

REFERENCES

1. Weilbaecher KN, Guise TA, McCauley LK (2011) Cancer to bone: a fatal attraction. Nat Rev Cancer 11:411-425
2. Cui D, Huang Z, Liu Y, Ouyang G (2017) The multifaceted role of periostin in priming the tumor microenvironments for tumor progression. Cell Mol Life Sci 74:4287-4291
3. Nakazawa Y, Taniyama Y, Sanada F, Morishita R, Nakamori S, Morimoto K, Yeung KT, Yang J (2018) Periostin blockade overcomes chemoresistance via restricting the expansion of mesenchymal tumor subpopulations in breast cancer. Sci Rep 8:4013
4. Brown JE, Cook RJ, Major P, Lipton A, Saad F, Smith M, Lee KA, Zheng M, Hei YJ, Coleman RE (2005) Bone turnover markers as predictors of skeletal complications in prostate cancer, lung cancer, and other solid tumors. J Natl Cancer Inst 97:59-69
5. Coleman R, Costa L, Saad F, Cook R, Hadji P, Terpos E, Garnero P, Brown J, Body JJ, Smith M, Lee KA, Major P, Dimopoulos M, Lipton A (2011) Consensus on the utility of bone markers in the malignant bone disease setting. Crit Rev Oncol Hematol 80:411-432
6. Liu AY, Zheng H, Ouyang G (2014) Periostin, a multifunctional matricellular protein in inflammatory and tumor microenvironments. Matrix Biol 37:150-156
7. Wu T, Wu S, Ouyang G (2014) Periostin: a new extracellular regulator of obesity-induced hepatosteatosis. Cell Metab 20:562-564
8. Venning FA, Wullkopf L, Erler JT (2015) Targeting ECM Disrupts Cancer Progression. Front Oncol 5:224
9. Bao S, Ouyang G, Bai X, Huang Z, Ma C, Liu M, Shao R, Anderson RM, Rich JN, Wang XF (2004) Periostin potently promotes metastatic growth of colon cancer by augmenting cell survival via the Akt/PKB pathway. Cancer Cell 5:329-339
10. Malanchi I, Santamaria-Martinez A, Susanto E, Peng H, Lehr HA, Delaloye JF, Huelsken J (2012) Interactions between cancer stem cells and their niche govern metastatic colonization. Nature 481:85-89
11. Merle B, Garnero P (2012) The multiple facets of periostin in bone metabolism. Osteoporos Int 23:1199-1212
12. Bonnet N, Standley KN, Bianchi EN, Stadelmann V, Foti M, Conway SJ, Ferrari SL (2009) The matricellular protein periostin is required for sost inhibition and the anabolic response to mechanical loading and physical activity. J Biol Chem 284:35939-35950
13. Gerbaix M, Vico L, Ferrari SL, Bonnet N (2015) Periostin expression contributes to cortical bone loss during unloading. Bone 71:94-100
14. Bonnet N, Conway SJ, Ferrari SL (2012) Regulation of beta catenin signaling and parathyroid hormone anabolic effects in bone by the matricellular protein periostin. Proc Natl Acad Sci U S A 109:15048-15053
15. Lipton A, Ali SM, Leitzel K, Demers L, Chinchilli V, Engle L, Harvey HA, Brady C, Nalin CM, Dugan M, Carney W, Allard J (2002) Elevated serum Her-2/neu level predicts decreased response to hormone therapy in metastatic breast cancer. J Clin Oncol 20:1467-1472
16. Rousseau JC, Sornay-Rendu E, Bertholon C, Chapurlat R, Garnero P (2014) Serum periostin is associated with fracture risk in postmenopausal women: a 7-year prospective analysis of the OFELY study. J Clin Endocrinol Metab 99:2533-2539
17. Rios H, Koushik SV, Wang H, Wang J, Zhou HM, Lindsley A, Rogers R, Chen Z, Maeda M, Kruzynska-Frejtag A, Feng JQ, Conway SJ (2005) periostin null mice exhibit dwarfism, incisor enamel defects, and an early-onset periodontal disease-like phenotype. Mol Cell Biol 25:11131-11144
18. Coutu DL, Wu JH, Monette A, Rivard GE, Blostein MD, Galipeau J (2008) Periostin, a member of a novel family of vitamin K-dependent proteins, is expressed by mesenchymal stromal cells. J Biol Chem 283:17991-18001

19. Annis DS, Ma H, Balas DM, Kumfer KT, Sandbo N, Potts GK, Coon JJ, Mosher DF (2015) Absence of Vitamin K-Dependent gamma-Carboxylation in Human Periostin Extracted from Fibrotic Lung or Secreted from a Cell Line Engineered to Optimize gamma-Carboxylation. PLoS One 10:e0135374
20. Contie S, Voorzanger-Rousselot N, Litvin J, Bonnet N, Ferrari S, Clezardin P, Garnero P (2010) Development of a new ELISA for serum periostin: evaluation of growth-related changes and bisphosphonate treatment in mice. Calcif Tissue Int 87:341-350
21. Contie S, Voorzanger-Rousselot N, Litvin J, Clezardin P, Garnero P (2011) Increased expression and serum levels of the stromal cell-secreted protein periostin in breast cancer bone metastases. Int J Cancer 128:352-360
22. Rousseau JC, Sornay-Rendu E, Bertholon C, Garnero P, Chapurlat R (2015) Serum periostin is associated with prevalent knee osteoarthritis and disease incidence/progression in women: the OFELY study. Osteoarthritis Cartilage 23:1736-1742
23. Sasaki H, Yu CY, Dai M, Tam C, Loda M, Auclair D, Chen LB, Elias A (2003) Elevated serum periostin levels in patients with bone metastases from breast but not lung cancer. Breast Cancer Res Treat 77:245-252
24. Sugiura T, Takamatsu H, Kudo A, Amann E (1995) Expression and characterization of murine osteoblast-specific factor 2 (OSF-2) in a baculovirus expression system. Protein Expr Purif 6:305-311
25. Novinec M, Lenarcic B (2013) Cathepsin K: a unique collagenolytic cysteine peptidase. Biol Chem 394:1163-1179
26. Bonnet N, Brun J, Rousseau JC, Duong LT, Ferrari SL (2017) Cathepsin K Controls Cortical Bone Formation by Degrading Periostin. J Bone Miner Res 32:1432-1441
27. Garnero P, Bonnet N, Ferrari SL (2017) Development of a New Immunoassay for Human Cathepsin K-Generated Periostin Fragments as a Serum Biomarker for Cortical Bone. Calcif Tissue Int
28. Hsu YH, Hsing CH, Li CF, Chan CH, Chang MC, Yan JJ, Chang MS (2012) Anti-IL-20 monoclonal antibody suppresses breast cancer progression and bone osteolysis in murine models. J Immunol 188:1981-1991
29. Littlewood-Evans AJ, Bilbe G, Bowler WB, Farley D, Wlodarski B, Kokubo T, Inaoka T, Sloane J, Evans DB, Gallagher JA (1997) The osteoclast-associated protease cathepsin K is expressed in human breast carcinoma. Cancer Res 57:5386-5390
30. Duong LT, Wesolowski GA, Leung P, Oballa R, Pickarski M (2014) Efficacy of a cathepsin K inhibitor in a preclinical model for prevention and treatment of breast cancer bone metastasis. Mol Cancer Ther 13:2898-2909
31. Stegemann C, Didangelos A, Barallobre-Barreiro J, Langley SR, Mandal K, Jahangiri M, Mayr M (2013) Proteomic identification of matrix metalloproteinase substrates in the human vasculature. Circ Cardiovasc Genet 6:106-117
32. Hou P, Troen T, Ovejero MC, Kirkegaard T, Andersen TL, Byrjalsen I, Ferreras M, Sato T, Shapiro SD, Foged NT, Delaisse JM (2004) Matrix metalloproteinase-12 (MMP-12) in osteoclasts: new lesson on the involvement of MMPs in bone resorption. Bone 34:37-47
33. Le Gall C, Bellahcene A, Bonnelye E, Gasser JA, Castronovo V, Green J, Zimmermann J, Clezardin P (2007) A cathepsin K inhibitor reduces breast cancer induced osteolysis and skeletal tumor burden. Cancer Res 67:9894-9902
34. Chen B, Platt MO (2011) Multiplex zymography captures stage-specific activity profiles of cathepsins K, L, and S in human breast, lung, and cervical cancer. J Transl Med 9:109
35. Kleer CG, Bloushtain-Qimron N, Chen YH, Carrasco D, Hu M, Yao J, Kraeft SK, Collins LC, Sabel MS, Argani P, Gelman R, Schnitt SJ, Krop IE, Polyak K (2008) Epithelial and stromal cathepsin K and CXCL14 expression in breast tumor progression. Clin Cancer Res 14:5357-5367
36. Tumminello FM, Flandina C, Crescimanno M, Leto G (2008) Circulating cathepsin K and cystatin C in patients with cancer related bone disease: clinical and therapeutic implications. Biomed Pharmacother 62:130-135

37. Garnero P, Grimaux M, Seguin P, Delmas PD (1994) Characterization of immunoreactive forms of human osteocalcin generated in vivo and in vitro. J Bone Miner Res 9:255-264
38. Rehder DS, Gundberg CM, Booth SL, Borges CR (2015) Gamma-carboxylation and fragmentation of osteocalcin in human serum defined by mass spectrometry. Mol Cell Proteomics 14:1546-1555

FIGURES LEGENDS

FIGURE 1: ELISA measurement of serum periostin levels in breast cancer patients with bone metastasis. (A): Schematic representation of AbH epitopes. **(B)** Serum periostin levels in women with breast cancer and bone metastasis (n = 53), compared with healthy age-matched postmenopausal women (n = 54). Data are shown using a box-and-whisker plot where boxes show the 25th, 50th (median) and 75th percentiles, and the ends of the whiskers indicate the 10th and 90th percentiles.

FIGURE 2: Identification of circulating periostin in Postn$^{+/+}$ and Postn$^{-/-}$ mice.

(A): Schematic representation of Ab1 and Ab2 antibody epitopes. All spliced variants of periostin share the amino-acid sequence recognized by Ab2 antibody, thereby allowing the detection of all periostin isoforms. SP= signal peptide; EMI= Emilin-like domain; FAS I= Fasciclin-like domain and CTR= C-terminal domain.

(B): Representative Western Blots of sera from Postn$^{+/+}$ and Postn$^{-/-}$ mice. The 1D electrophoresis was performed under non-reducing (-DTT) or reducing (+DTT) conditions on 7.5% SDS-polyacrylamide gels. The proteins were transferred to nitrocellulose membranes and immunoblotted with anti-periostin Ab1 or Ab2 antibodies. Arrows show periostin-positive bands.

(C): Representative Western Blots of serum from Postn$^{+/+}$ mouse. The 1D electrophoresis and the immunoblotting were performed as described in (B). Then a single lane was split in half (dotted line), each half was blotted separately with antibodies Ab1 or Ab2, and the two halves were matched prior to imaging.

FIGURE 3: Expression of intact and truncated forms of periostin in the serum and tissues (bone, lung, heart) of Postn$^{+/+}$ and Postn$^{-/-}$ mice.

Representative 2D electrophoresis patterns of Postn $^{+/+}$ and Postn $^{-/-}$ mouse serum and tissues immunoblotted with Ab1 and Ab2 antibodies.

(A): Ab1 antibody. For Postn $^{+/+}$ mice, box 1: Ab1-positive spots with pI ranged between 6 and 7; box 2: Ab1-positive spots with pI ranged between 7 and 9 and box 3: Ab1-positive spots with truncated periostin forms. Negative control with Postn $^{-/-}$ mice: arrows show nonspecific Ab1-positive spots.

(B): Ab2 antibody. For Postn $^{+/+}$ mice, box 2: Ab2-positive spots with pI ranged between 7 and 9; boxes 1 and 3: absence of periostin spots with Ab2. Negative control with Postn $^{-/-}$ mice: arrows show nonspecific Ab2-positive spots.

(C): Postn $^{+/+}$ mouse serum: magnification of boxes 1 and 2.

FIGURE 4: Expression of γ-carboxylated proteins in the serum and tissues (bone, lung) of Postn$^{+/+}$ and Postn$^{-/-}$ mice.

Representative 2D electrophoresis patterns of serum and tissues from Postn $^{+/+}$ and Postn $^{-/-}$ mice immunoblotted with an anti-Gla monoclonal antibody. Boxes 1, 2 and 3 correspond to periostin-positive regions. Gla-positive spots were more acidic and did not overlap with periostin-positive regions. Additionally, similar arrays of Gla-positive spots in the serum and tissues (bone, lung) from Postn$^{+/+}$ and Postn$^{-/-}$ mice were observed.

FIGURE 5: HIC of normal and metastatic bones.

(A): Representative immunostaining of normal bone with anti-periostin Ab1 and Ab2 antibodies. A strong staining was observed in the periosteum (arrows).

(B): Representative immunostaining of 4T1 breast cancer metastatic bone tissue sections with anti-periostin Ab1 and Ab2 antibodies, Cathepsin K antibody and TRAP staining. A strong staining was observed at the tumor-bone interface with Ab1. There was no staining at the tumor-bone interface with Ab2. As judged by TRAP staining, osteoclasts were present at the tumor-bone interface. Osteoclasts are stained red. Immunostaining for cathepsin K co-localized with TRAP staining.

(C): Representative immunostaining with Ab1 or Ab2 antibody (upper and lower panels, respectively) of the periosteum (arrows) in normal bone areas at a distance from skeletal tumors (*). Both antibodies stained the periosteum.

FIGURE 6: Measurement of serum periostin levels in a mouse model of breast cancer bone metastasis.

(A): Standard curve of the mouse periostin sandwich immunoassay. The x–axis corresponds to serial dilutions of a known concentration of recombinant mouse periostin, used here as a standard. The y-axis shows the optical density (OD). The detection limit -defined as the concentration 2 standard deviations above that of the lowest calibrator- was <1 ng/ml. Serum periostin was stable for up to 5 thaw/freeze cycles and at least 2 hrs at room temperature.

(B): Serum periostin levels in animals bearing osteolytic lesions (n = 9), 2 weeks after inoculation of murine 4T1 breast cancer cells, compared with naïve animals that did not receive 4T1 cells (n = 9). Inset: Representative radiographic image of mouse metastatic legs, showing the extent of bone destruction (arrows).

FIGURE 7: Periostin is a substrate for cathepsin K.

(A): Representative immunoblots of mouse recombinant periostin not treated (-) or treated with cathepsin K (+) (cathepsin K/ periostin ratio 0.5). The 1D electrophoresis was performed under reducing condition on 4-20% SDS-polyacrylamide gels. The proteins were transferred to nitrocellulose membranes and immunoblotted with anti-periostin Ab1 or Ab2 antibodies. Alternatively, the electrophoresed proteins were stained with Coomassie blue directly in the gel. Both Ab1 and Ab2 antibodies recognized the intact form of periostin, whereas truncated forms of periostin were detected by Ab1 antibody only. The proteolytic degradation of periostin by cathepsin K generated a 25-kDa Coomassie-blue stained band (arrow) that was extracted from the gel and subjected to LC-MS/MS analysis.

(B): Amino acid sequence of the 25-kDa Coomassie-blue stained band, starting from residue Val97 to residue Glu377 (in boldface type and underlined).

(C): Schematic representation of periostin domain structure, highligting the two first FAS I domains which correspond to the amino acid sequence of the 25-kDa proteolytic fragment generated by cathepsin K. As opposed to Ab2 antibody, Ab1 antibody binds to this proteolytic fragment.

(D): A representative immunoblots of mouse recombinant periostin treated or not with different ratio of cathepsin K / periostin (0.5, 0.1, 0.01). The 1D electrophoresis was performed under reducing condition on 4-20% SDS polyacrylamide gels. The proteins were transferred to a nitrocellulose membrane and immunoblotted with antiperiostin Ab1 and Ab2 antibodies. In the table was reported the % of iPTN measured with the specific ELISA according to the cathepsin K/ periostin ratio.

Figure 1

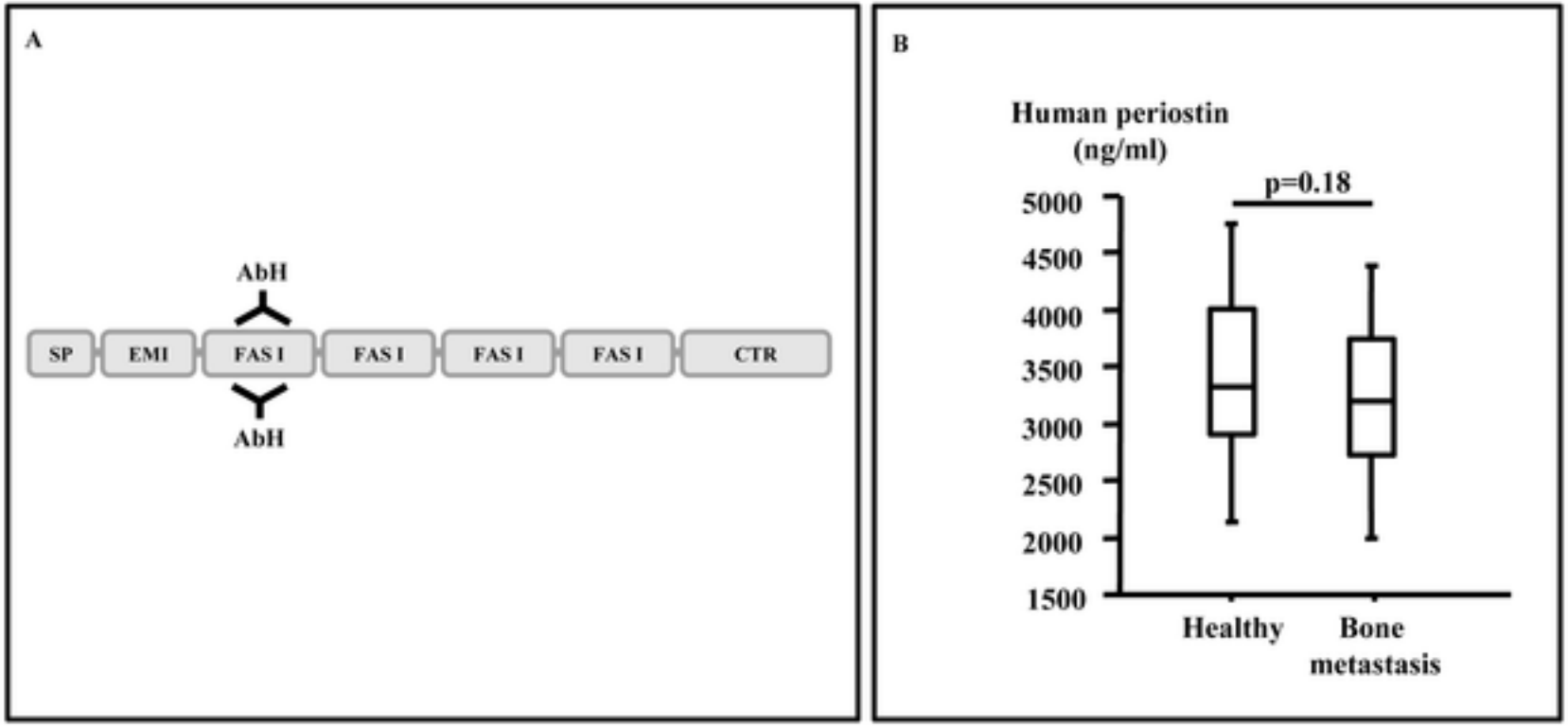

Figure 2

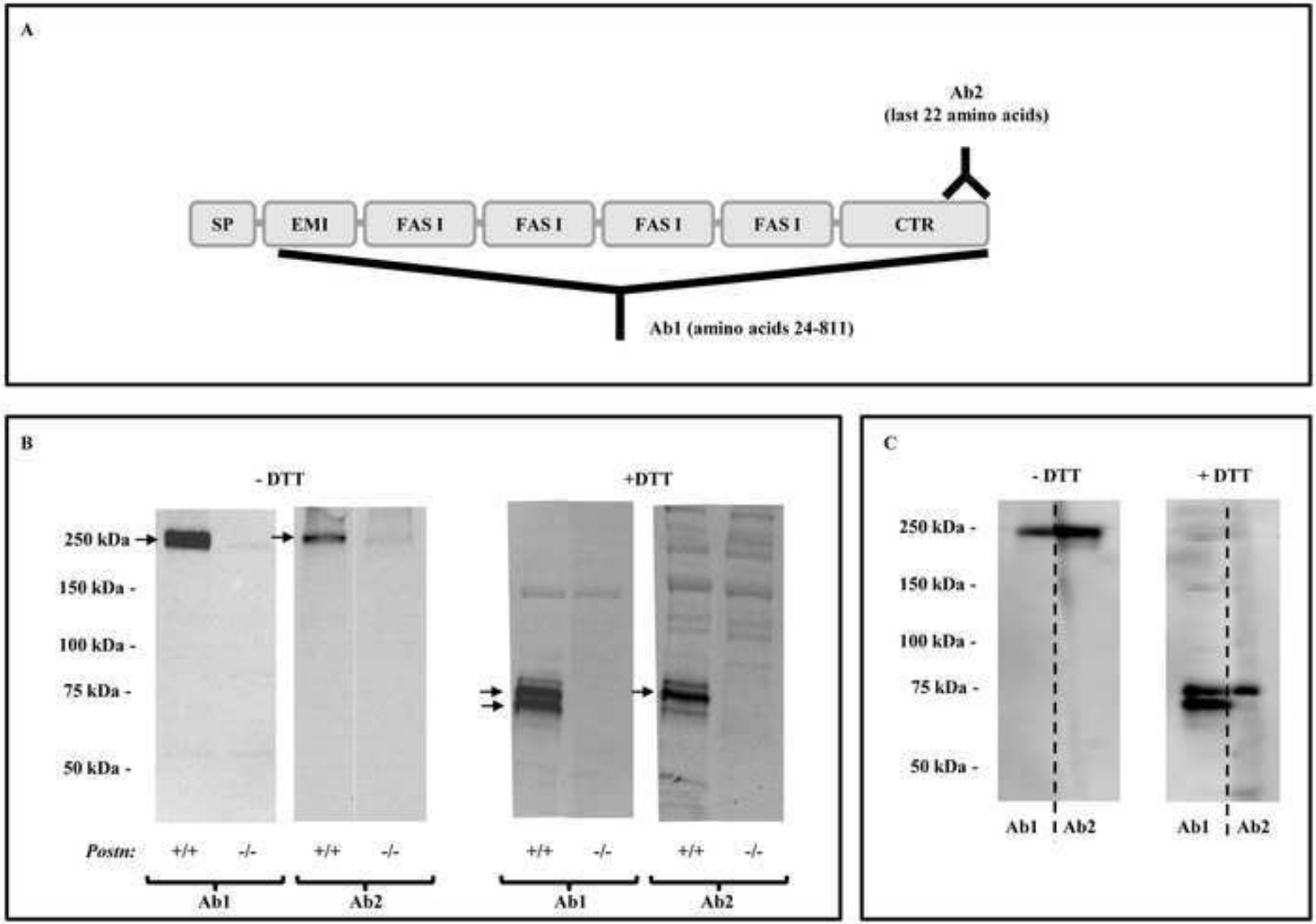

Figure 3

Click here to download Figure Fig3.tif

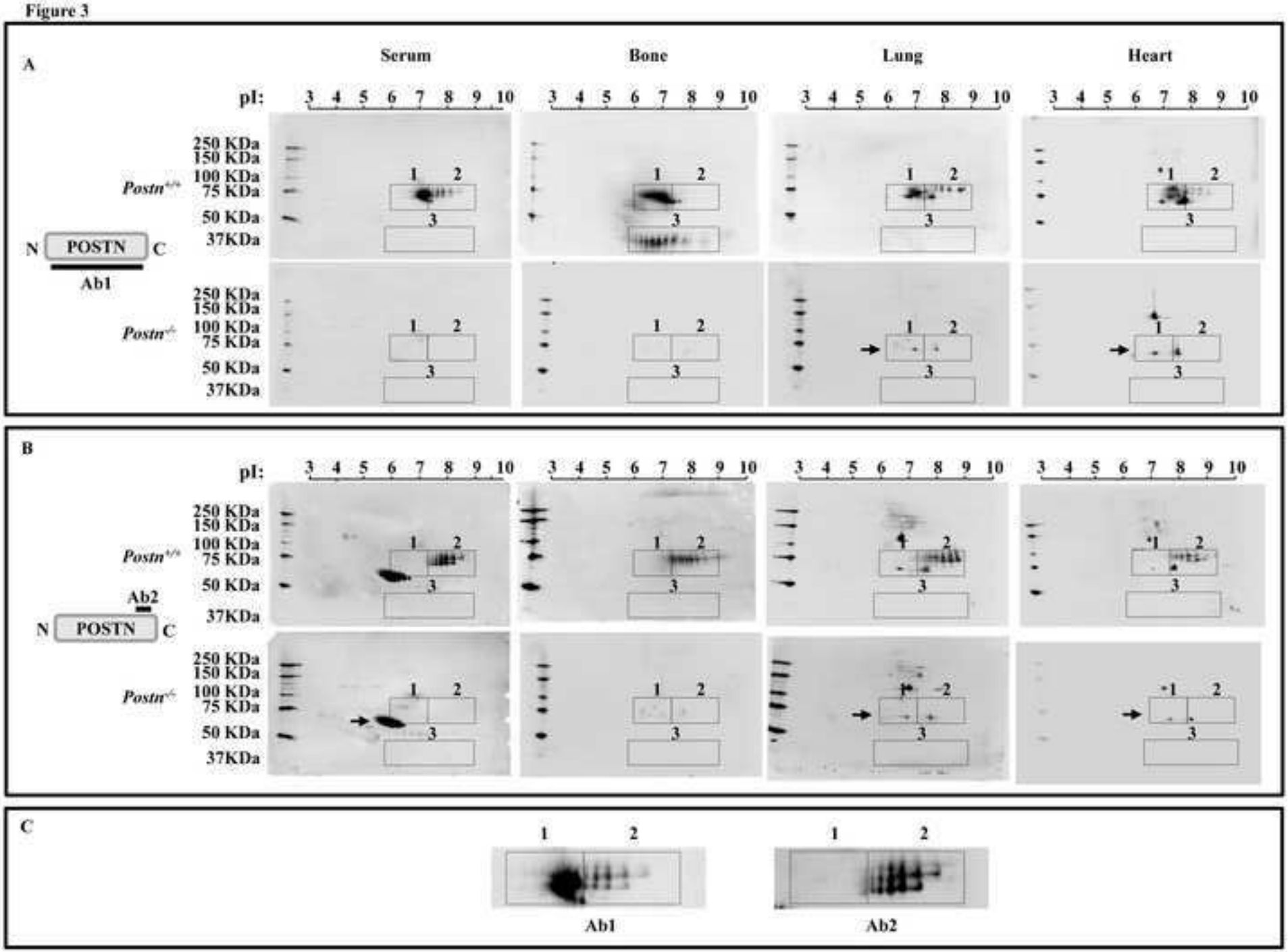

Figure 4

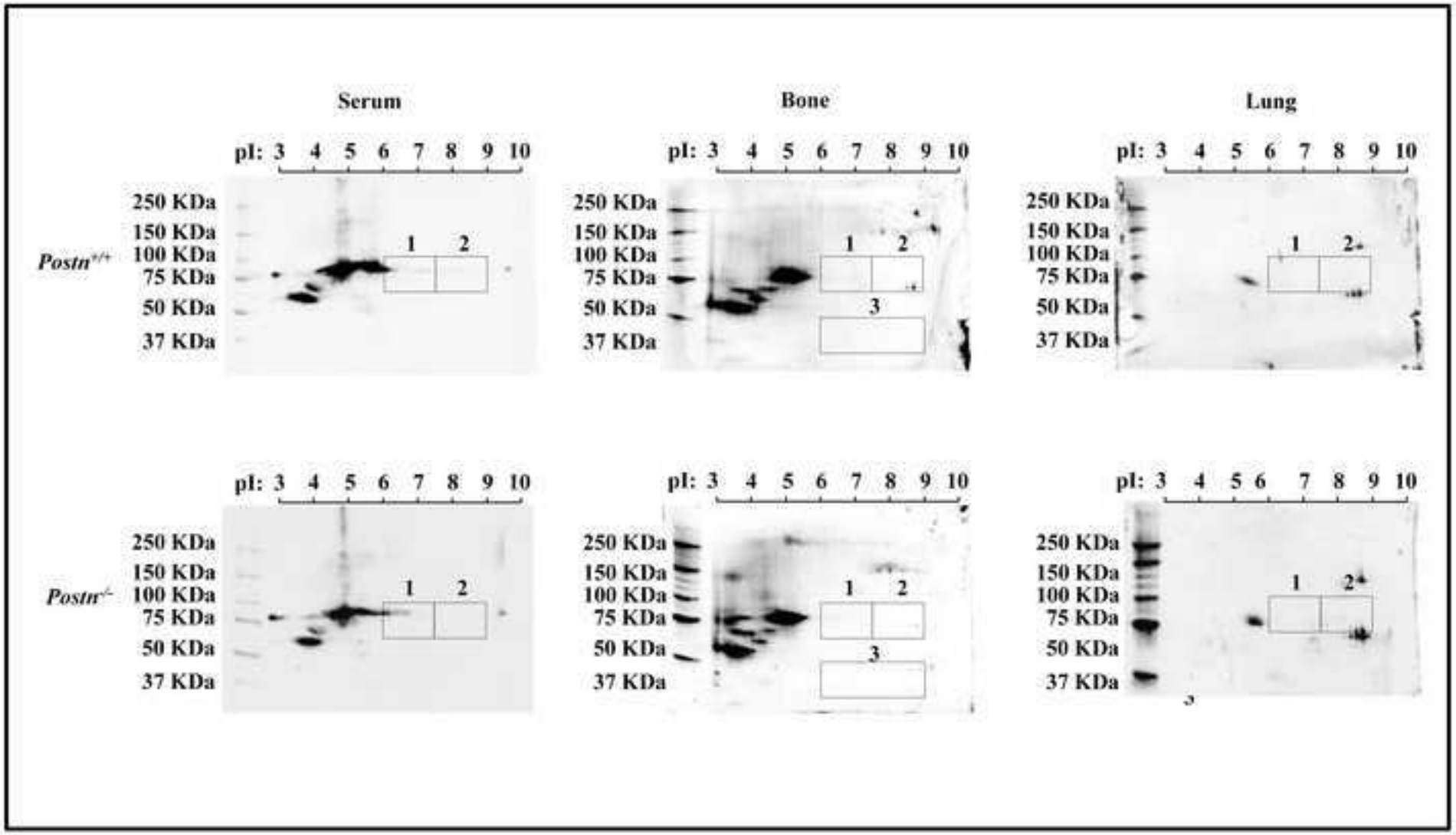

Figure 5

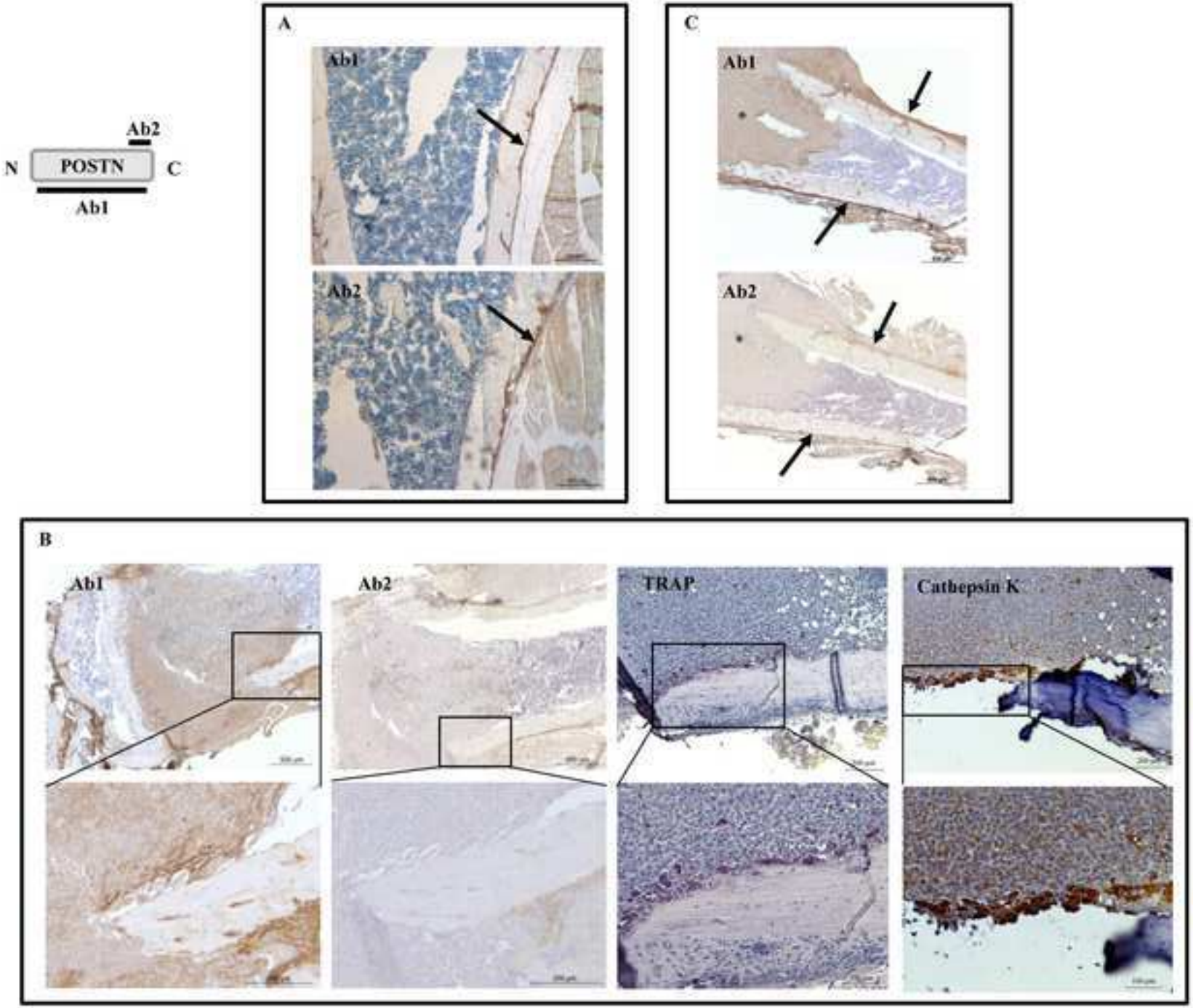

Figure 6

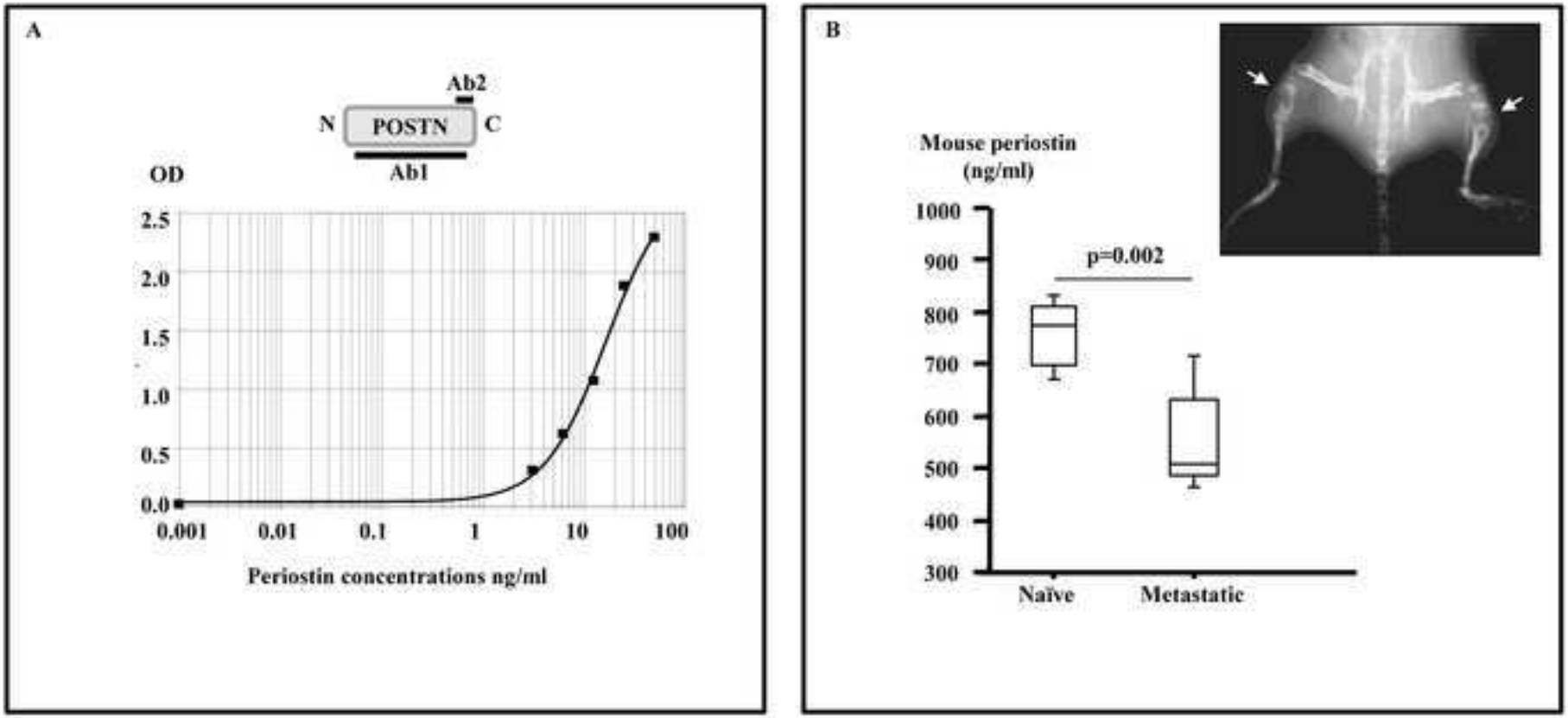

Figure 7

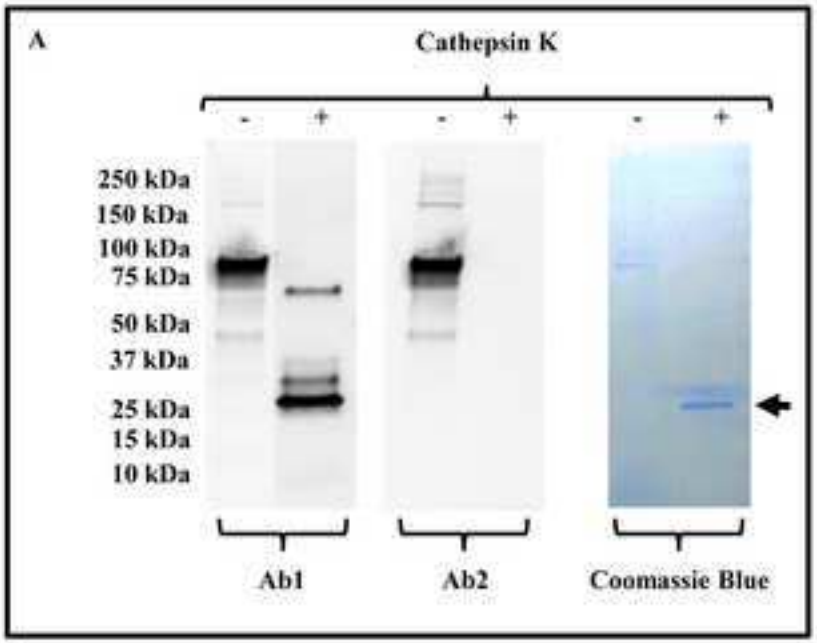

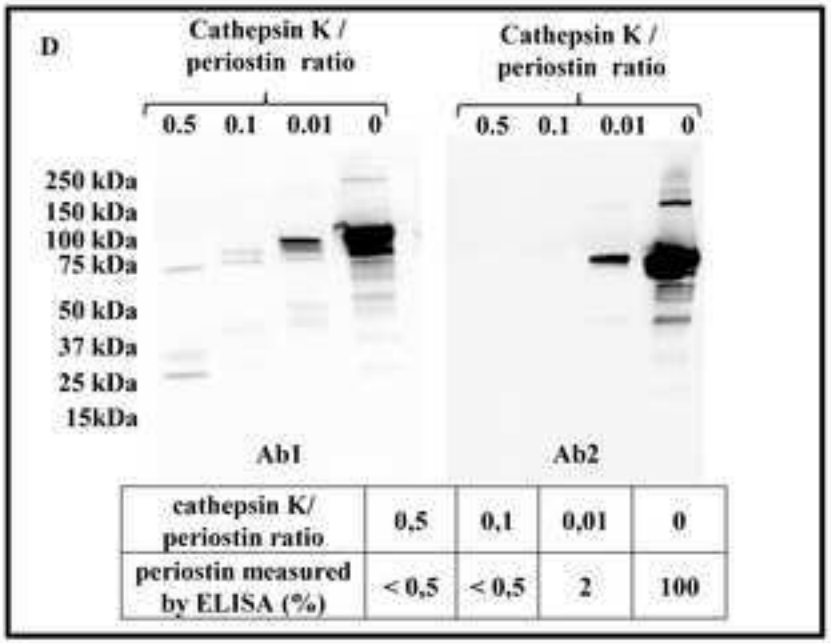

cathepsin K/ periostin ratio	0,5	0,1	0,01	0
periostin measured by ELISA (%)	< 0,5	< 0,5	2	100

B

```
 24 NSYYDKVLAH SRIRGRDQGP NVCALQQILG TKKKYFSSCK NWYQGAICGK KTTVLYECCP GYMRMEGMKG CPAVMPIDHV
104 YGTLGIVGAT TTQHYSDVSK LREEIEGKGS YTYFAPSNEA WENLDSDIRR GLENNVNVEL LNALHSHMVN KRMLTKDLKH
184 GMVIPSMYNN LGLFINHYPN GVVTVNCARV IHGNQIATNG VVHVIDRVLT QIGTSIQDFL EAEDDLSSFR AAAITSDLLE
264 SLGRDGHFTL FAPTNEAFEK LPRGVLERIM GDKVASEALM KYHILNTLQC SEAITGGAVF ETMEGNTIEI GCEGDSISIN
344 GIKMVNKKDI VTKNGVIHLI DEVLIPDSAK QVIELAGKQQ TTFTDLVAQL GLASSLKPDG EYTLLAPVNN AFSDDTLSMD
424 QRLLKLILQN HILKVKVGLS DLYNGQILET IGGKQLRVFV YRTAICIENS CMVRGSKQGR NGAIHIFREI IQPAEKSLHD
504 KLRQDKRFSI FLSLLEAADL KDLLTQPGDW TLFAPTNDAF KGMTSEEREL LIGDKNALQN IILYHLTPGV YIGKGFEPGV
584 TNILKTTQGS KIYLKGVNET LLVNELKSKE SDIMTTNGVI HVVDKLLYPA DIPVGNDQLL ELLNKLIKYI QIKFVRGSTF
664 KEIPMTVYRP AMTKIQIEGD PDFRLIKEGE TVTEVIHGEP VIKKYTKIID GVPVEITEKQ TREERIITGP EIKYTRISTG
744 GGETGETLQK FLQKEVSKVT KFIEGGDGHL FEDEEIKRLL QGDTPAKKIP ANKRVQGPRR RSREGRSQ
```

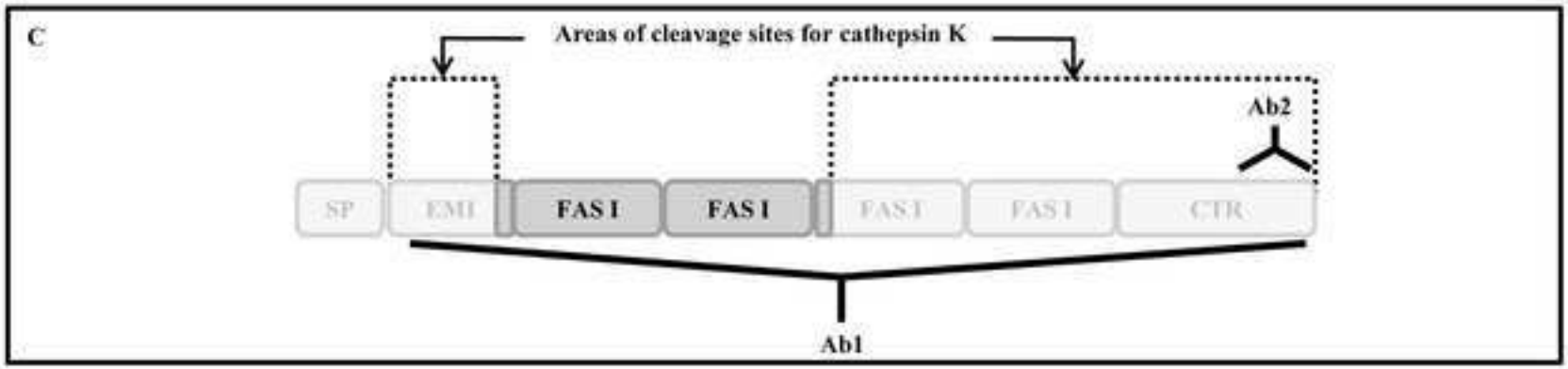

Figure S1

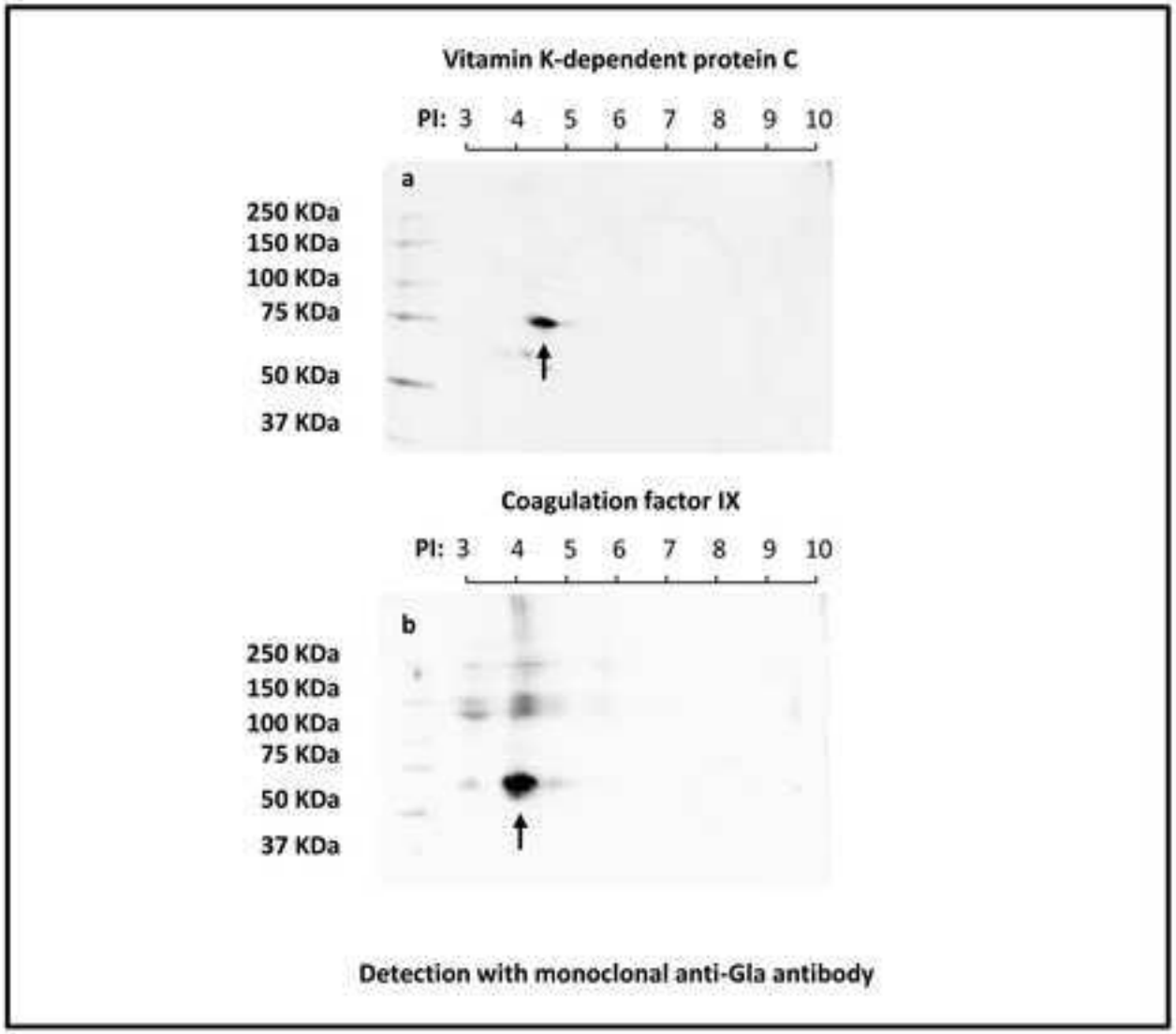

Figure S2